Eur Arch Otorhinolaryngol (2015) 272:3821–3824
DOI 10.1007/s00405-014-3467-7

HEAD AND NECK

# High-resolution three-dimensional diffusion-weighted MRI/CT image data fusion for cholesteatoma surgical planning: a feasibility study

**Koji Yamashita · Akio Hiwatashi · Osamu Togao · Kazufumi Kikuchi · Nozomu Matsumoto · Makoto Obara · Takashi Yoshiura · Hiroshi Honda**

Received: 7 October 2014 / Accepted: 19 December 2014 / Published online: 28 December 2014


**Abstract** The aim of the study was to assess the feasibility of high-resolution three-dimensional diffusion-weighted images (HR3D-DWIs)/multi-detector row CT (MDCT) images' data fusion for surgical planning for cholesteatoma. A total of 12 patients (7 male and 5 female; age range 11–72 years; mean 38.1 years) with cholesteatoma underwent preoperative MRI using a 3.0-T clinical unit and an 8-channel array-head coil. For each subject, HR3D-DWIs were obtained using a turbo field-echo with diffusion-sensitized driven-equilibrium preparation with 1.5 mm iso-voxel dimension. These patients also underwent MDCT with a slice thickness of 0.5 mm. Fusion of the HR3D-DWIs and MDCT images was performed using an automated rigid registration and subsequent manual fine-tuning by a board-certified neuroradiologist on a workstation. Fused images were compared to CT and findings confirmed based on operation reports. On the fused images, the extent of the cholesteatoma, which was depicted as a conspicuous high-intensity lesion could be easily evaluated with background bony structures. In all patients, the location and extent of the cholesteatoma on the fused images corresponded well with the intraoperative findings. Image fusion between HR3D-DWIs and MDCT images is feasible, and provides valuable preoperative information for surgical planning to otorhinolaryngologists.

**Keywords** Cholesteatoma · Three-dimensional image · Temporal bone · Diffusion-weighted MRI · Computed tomography

K. Yamashita (✉) · A. Hiwatashi · O. Togao · K. Kikuchi · T. Yoshiura · H. Honda
Department of Clinical Radiology, Graduate School of Medical Sciences, Kyushu University, 3-1-1 Maidashi, Higashi-ku, Fukuoka 812-8582, Japan
e-mail: yamakou@radiol.med.kyushu-u.ac.jp

N. Matsumoto
Department of Otorhinolaryngology, Graduate School of Medical Sciences, Kyushu University, Fukuoka, Japan

M. Obara
Philips Electronics Japan, Tokyo, Japan

## Introduction

Diffusion-weighted imaging (DWI) is diagnostic in middle ear cholesteatoma [1–5]. Cholesteatomas are visualized as a conspicuously hyperintense lesion on DWI. It is postulated that restricted free water molecular diffusion, the T2 "shine-through" effect, or a combination of both is responsible for the marked hyperintensity. The main drawback of this method is a lack of visualization of bony structures. In contrast, multi-detector row CT (MDCT) has the advantage of high-resolution imaging of bony structures, while it is difficult to distinguish cholesteatoma from granulation tissue, fibrous tissue or fluid [6–8]. Combining the advantages of the DWI/MDCT, fused image would comprehensively display the location and extent of the cholesteatoma, thereby help preoperative planning [9]. Recently, high-resolution 3D diffusion-weighted images based on turbo field-echo with diffusion-sensitized driven-equilibrium (TFE-DSDE) have been developed for the imaging of middle ear cholesteatoma [1]. With minimal image distortion and high-resolution 3D iso-voxel data acquisition, TFE-DSDE images could be easily compared with high-resolution CT images. Therefore, our purpose was to assess the feasibility of TFE-DSDE/MDCT images' data fusion for surgical planning for cholesteatoma.

## Materials and methods

### Case selection

This study was approved by the institutional review board of our hospital. Informed consent for study participation was waived due to the retrospective nature of this study. The consecutive patients obtained between February 2011 and February 2012 were retrospectively analyzed. A total of 12 patients (7 male and 5 female; age range 11–72 years; mean 38.1 years) with unilateral cholesteatoma (8 primary and 4 recurrent) underwent preoperative MRI and CT. Each patient underwent preoperative MRI on the day before surgery. The mean time interval between MR and CT imaging was 39 days (range 0–90 days).

### Imaging techniques

Each patient underwent TFE-DSDE using a 3.0-T MR unit (Achieva Quasar Dual, Philips Medical Systems, Best, The Netherlands) and an 8-channel array-head coil. The TFE-DSDE sequence has two distinct components: the DSDE preparation and the segmented 3D TFE data acquisition. Adiabatic refocusing pulses and additional gradients inserted in front of the sequence were used to reduce B0 and B1 inhomogeneity, and eddy current effects [10–13]. Data acquisition using 3D segmented gradient echo (TFE) was performed immediately after the DSDE preparation. To eliminate T1 effects in the signal acquired by the TFE, we used a phase cycling scheme [14, 15]. The detailed description of the sequence has been described elsewhere [1]. The imaging parameters used for TFE-DSDE were as follows: 24 transverse slices, TR/TE = 6.2/3 ms, FA = 10°, echo train length = 75, b factor = 800 s/mm$^2$, SENSE factor = 2, FOV = 240 mm, voxel size = 1.5 × 1.5 × 1.5 mm$^3$, number of signal averages = 2, and acquisition time = 2 min 40 s.

The patients also underwent CT images of temporal bone using a 64-detector-row CT scanner (Aquilion, Toshiba Medical Systems Corporation, Tochigi, Japan) with 0.5-mm collimation and a 512 × 512 matrix. Transverse scans were acquired parallel to the orbitomeatal plane in the helical mode using the following parameters: 120 kV, 250 mAs, 1-s rotation time, 0.5-mm section thickness, beam pitch of 0.625, and field of view of 240 mm. The obtained image data were displayed at a window center of 400 HU and a window width of 4,000 HU.

### Registration of TFE-DSDE and CT data

Fusion of TFE-DSDE and CT images was performed by automated rigid registration and subsequent manual fine-tuning by a board-certified neuroradiologist on Synapse Vincent (Fujifilm, Tokyo, Japan). Fused images were created by overlaying TFE-DSDE images onto the semi-transparent CT images. In the manual fine-tuning, TFE-DSDE images were translated and rotated relative to the semi-transparent CT images.

### Image evaluation

Images of the 12 patients (12 temporal bones) were reviewed by two independent neuroradiologists with, respectively, 13 and 15 years of experience in head and neck radiology, who were blinded to the patients' clinical information. The two neuroradiologists independently evaluated the extent of cholesteatoma in two separate reading sessions. They read CT images alone (session 1) and TFE-DSDE/CT fusion images (session 2), respectively. In each reading session, the neuroradiologists reported the involved sites (attic, antrum, middle ear, mastoid, Eustachian tube, and labyrinth) of cholesteatoma [16]. The extent of cholesteatoma determined in each reading session was compared with surgical findings.

### Statistical analyses

The interobserver agreement on the rating was evaluated using the $\kappa$ statistics. The accuracy of the extent of cholesteatoma was compared between CT and TFE-DSDE/CT fused image using McNemar's test. In addition, Mann–Whitney $U$ test was used to compare the average number of involved sites between CT and TFE-DSDE/CT fusion images. Statistical analyses were performed using JMP 9 software (SAS Institute, Cary, NC). In all statistical analyses, the level of significance was set at $p < 0.05$.

## Results

Table 1 summarizes the results of the observer test. Excellent interobserver agreement was shown for the fused images ($\kappa = 0.881$), whereas fair agreement was obtained for the CT images ($\kappa = 0.390$). The fused images were associated with significantly higher accuracy (87.5 %) in estimating the cholesteatoma extent compared to CT (accuracy = 29.2 %) ($p = 0.0002$). The average number of involved sites (3.25 ± 1.33) was significantly higher

**Table 1** Average number ± SD (range) of involved sites per case

| CT | Fused image | Intraoperative findings |
|---|---|---|
| 3.25 ± 1.33 (1–5) | 2.17 ± 1.13 (1–4) | 2.17 ± 1.19 (1–4) |

The numbers on the list indicate the average of the two observers' data

with CT images than with the fused images (2.17 ± 1.13) and the intraoperative findings (2.17 ± 1.19) ($p < 0.05$, respectively). No significant difference was found between the fused images and the intraoperative findings. Figure 1a–e displays the illustrative case.

## Discussion

It is important to identify the precise extent of cholesteatoma and anatomic landmarks preoperatively to choose the correct surgical procedure [17]. In some institutions, an endoscopic surgery through the external ear canal is selected, instead of wide mastoid drilling, to manage cholesteatomas of limited extension [18]. The minimally invasive, but narrow-access endoscopic surgery requires precise preoperative evaluation of the location and extent of cholesteatoma. DWI and CT images can provide complementary information for this purpose [1–9]. Our study showed that the location and extent of the cholesteatoma on the fused images corresponded well with the intraoperative findings. To our best knowledge, this is the first report demonstrating the feasibility of high-resolution 3D DWI/CT fusion image for the preoperative assessment of temporal bone cholesteatoma. The most widely used acquisition technique for DWI is single-shot echo-planar imaging (SS-EPI). SS-EPI suffers from strong susceptibility artifacts in the skull base imaging. TFE-DSDE was developed to mitigate this problem. A previous report

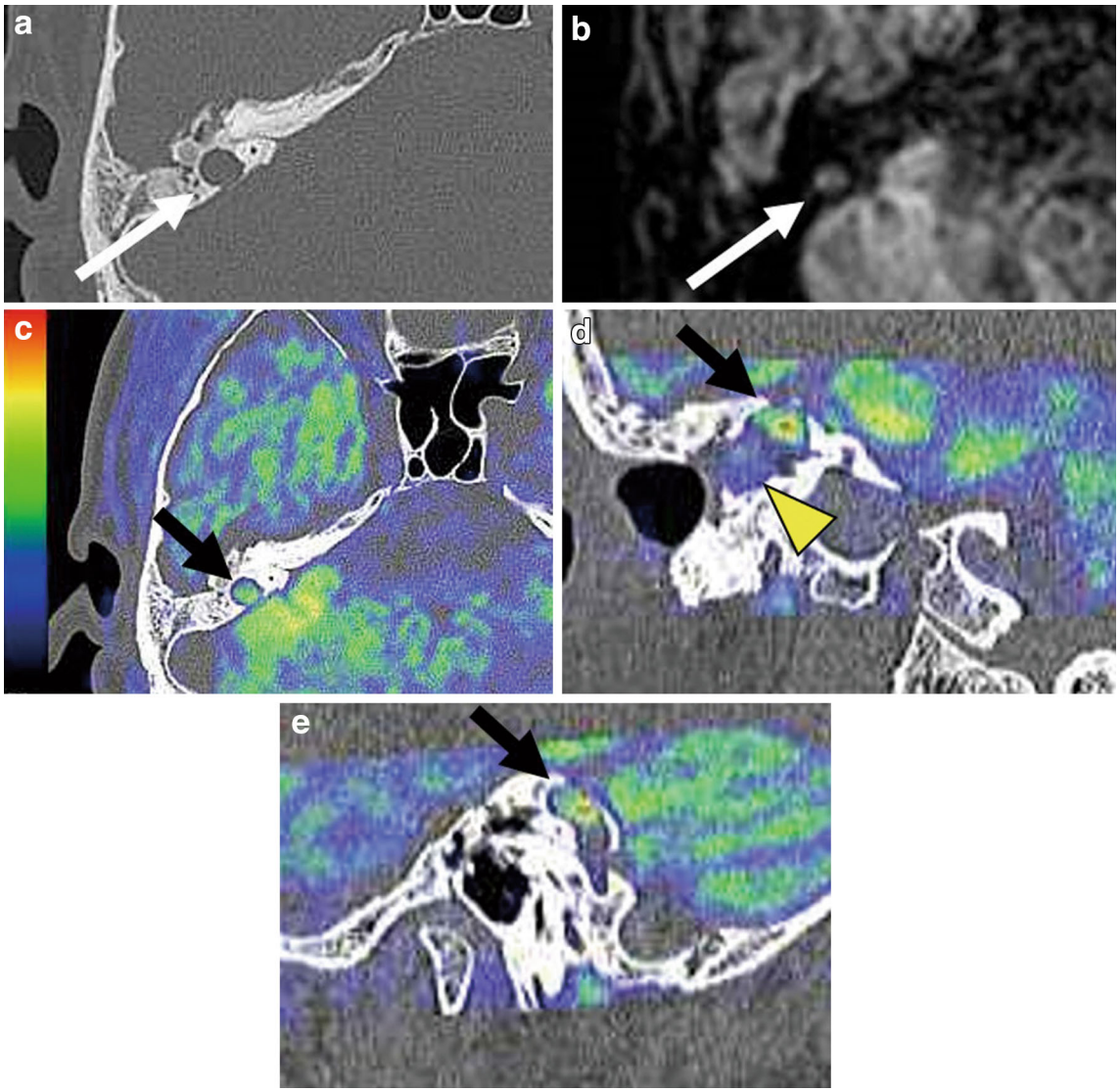


**Fig. 1** A 38-year-old male with recurrent cholesteatoma in the right middle ear. **a** CT, **b** TFE-DSDE, **c** axial fused image, **d** coronal fused image, **e** sagittal fused image. On CT, a low-density lesion is located in the supralabyrinth. On TFE-DSDE, a nodular lesion with hyperintensity suggestive of cholesteatoma is visualized (*arrow*). 3D fused image showing the *yellow*/*red* colored lesion corresponds to the low-density lesion on CT. A cholesteatoma was found during the subsequent surgery. The laterally located lesion is visualized as a blue spot on fused image (*arrowhead*). Granulomatous tissues were surgically proven

has shown that TFE-DSDE was associated with significantly higher sensitivity and accuracy than conventional SS-EPI DWI in detecting temporal bone cholesteatoma [1]. Furthermore, TFE-DSDE is capable of high-resolution 3D isovoxel acquisition, which makes it suitable for fusion with high-resolution CT images.

The fused image was associated with significantly higher accuracy and better interobserver agreement in evaluating the extent of cholesteatoma compared to CT image alone. We speculate that this improvement is due to improved specificity in tissue characterization provided by DWI. This speculation is confirmed by our findings that the number of involved sites was overestimated with CT whereas no such overestimation was observed with the fused images (Table 1).

It is important to know the comparison of fused images to DWI alone. However, the comparison was difficult and problematic due to the lack of bony anatomic landmarks.

Our study has several limitations. First, although the spatial resolution of our TFE-DSDE sequence (1.5 mm isovoxel) is higher than that of the conventional DWI sequence, it is still substantially lower than that of high-resolution CT (approximately 0.5 mm iso-voxel). Second, an automated rigid registration technique used for image fusion often required subsequent fine manual adjustment to achieve satisfactory results. Other registration methods such as rigid landmark technique [19] might improve the precision. Third, the intervals between CT and MRI examinations were relatively long (mean 39 days), although MRI was obtained on the day before the surgery in each patient. Finally, the number of patients was relatively few. Further studies involving larger number of patients are needed to establish our proposed method.

## Conclusions

Our results demonstrated that image fusion between TFE-DSDE and MDCT is feasible. It may provide valuable preoperative information for surgical planning to otorhinolaryngologists.

**Conflict of interest** Publication is approved by all authors and explicitly by the responsible authorities where the work was carried out. KY, AH, OT, KK, NM, TY, HH: none. MO: Philips employee.

## References


1. Yamashita K, Yoshiura T, Hiwatashi A et al (2013) High-resolution three-dimensional diffusion-weighted imaging of middle ear cholesteatoma at 3.0 T MRI: usefulness of 3D turbo field-echo with diffusion-sensitized driven-equilibrium preparation (TFE-DSDE) compared to single-shot echo-planar imaging. Eur J Radiol 82(9):e471–e475
2. Dubrulle F, Souillard R, Chechin D et al (2006) Diffusion weighted MR imaging sequence in the detection of postoperative recurrent cholesteatoma. Radiology 238(2):604–610
3. Lehmann P, Saliou G, Brochart C et al (2009) 3T MR imaging of postoperative recurrent middle ear cholesteatomas: value of periodically rotated overlapping parallel lines with enhanced reconstruction diffusion-weighted MR imaging. AJNR Am J Neuroradiol 30(2):423–427
4. De Foer B, Vercruysse JP, Bernaerts A et al (2010) Middle ear cholesteatoma: non-echo-planar diffusion-weighted MR imaging versus delayed gadolinium-enhanced T1-weighted MR imaging—value in detection. Radiology 255(3):866–872
5. Yamashita K, Yoshiura T, Hiwatashi A et al (2011) Detection of middle ear cholesteatoma by diffusion-weighted MR imaging: multi-shot echo-planar imaging compared to single-shot echo-planar imaging. AJNR Am J Neuroradiol 32(10):1915–1918
6. Jackler RK, Dillon WP, Schindler RA (1984) Computed tomography in suppurative ear disease: a correlation of surgical and radiographic findings. Laryngoscope 94(6):746–752
7. Yates PD, Flood LM, Banerjee A, Clifford K (2002) CT scanning of middle ear cholesteatoma: what does the surgeon want to know? Br J Radiol 75(898):847–852
8. Yamashita K, Yoshiura T, Hiwatashi A et al (2011) Contributing factors in the pathogenesis of acquired cholesteatoma: size analysis based on MDCT. AJR Am J Roentgenol 196(5):1172–1175
9. Plouin-Gaudon I, Bossard D, Ayari-Khalfallah S, Froehlich P (2010) Fusion of MRIs and CT scans for surgical treatment of cholesteatoma of the middle ear in children. Arch Otolaryngol Head Neck Surg 136(9):878–883
10. Obara M, Takahara T, Honda M, Kwee T, Imai Y, Van Cauteren M (2011) Diffusion weighted MR nerve sheath imaging (DW-NSI) using diffusion-sensitized driven-equiliblium (DSDE) In: Proceedings of the joint annual meeting ISMRM-ESMRMB, Montreal, Canada, p 4023
11. Nezafat R, Stuber M, Ouwerkerk R, Gharib AM, Desai MY, Pettigrew RI (2006) B1-insensitive T2 preparation for improved coronary magnetic resonance angiography at 3 T. Magn Reson Med 55(4):858–864
12. Jeong EK, Kim SE, Parker DL (2003) High-resolution diffusion-weighted 3D MRI, using diffusion-weighted driven-equilibrium (DW-DE) and multishot segmented 3D-SSFP without navigator echoes. Magn Reson Med 50(4):821–829
13. Wang J, Yarnykh VL, Yuan C (2010) Enhanced image quality in black-blood MRI using the improved motion-sensitized driven-equilibrium (iMSDE) sequence. J Magn Reson Imaging 31(5):1256–1263
14. Coremans J, Spanoghe M, Budinsky L et al (1997) A comparison between different imaging strategies for diffusion measurements with the centric phase-encoded turboFLASH sequence. J Magn Reson 124(2):323–342
15. Thomas DL, Pell GS, Lythgoe MF, Gadian DG, Ordidge RJ (1998) A quantitative method for fast diffusion imaging using magnetization-prepared turboFLASH. Magn Reson Med 39(6):950–960
16. Saleh HA, Mills RP (1999) Classification and staging of cholesteatoma. Clin Otolaryngol Allied Sci 24(4):355–359
17. Nemec SF, Donat MA, Mehrain S et al (2007) CT–MR image data fusion for computer assisted navigated neurosurgery of temporal bone tumors. Eur J Radiol 62(2):192–198
18. Tarabichi M, Nogueira JF, Marchioni D, Presutti L, Pothier DD, Ayache S (2013) Transcanal endoscopic management of cholesteatoma. Otolaryngol Clin N Am 46(2):107–130
19. Yamashita K, Yoshiura T, Hiwatashi A, Kamano H, Honda H (2012) Ultrashort echo time imaging of middle ear ossicles: a feasibility study. Dentomaxillofac Radiol 41(7):601–604